

On the Convex Parametrization of Spacecraft Orientation in Presence of Constraints and its Applications*

Yoonsoo Kim[†]

Department of Mechanical & Mechatronic Engineering
University of Stellenbosch, South Africa

Mehran Mesbahi[‡]

Department of Aeronautics & Astronautics
University of Washington
Seattle, WA 98195

Gurkirpal Singh[§] and Fred Y. Hadaegh[¶]

Jet Propulsion Laboratory
California Institute of Technology
Pasadena, CA 91109

Abstract

Guiding the rotational motion of a spacecraft subject to constraints on its permissible orientation often leads to non-convex optimal control problems. In this paper, we consider convex parametrizations of sets associated with the constrained rigid body orientations. We then elaborate on ramifications of such a parametrization in the development of guidance laws for autonomous spacecraft re-orientation that are based on convex optimization algorithms. These guidance problems appear in almost every space science mission equipped with heat or light sensitive instruments, e.g., cryogenically cooled infrared telescopes, star trackers, and low energy ion composition analyzers. The paper concludes with an example, demonstrating the viability of the proposed algorithm for constrained multiple spacecraft re-orientations.

*June 2007.

[†]Senior Lecturer, Email: ykim@sun.ac.za

[‡]Corresponding author. Associate Professor. Email: mesbahi@aa.washington.edu

[§]Senior Technical Staff. Email: gurkirpal.singh@jpl.nasa.gov

[¶]Senior Research Scientist. Email: fred.y.hadaegh@jpl.nasa.gov

Nomenclature

R	= real numbers
Rⁿ	= n -dimensional Euclidean space
R^{m×n}	= $m \times n$ real matrices
I_n	= $n \times n$ identity matrix
$0_{m \times n}$	= $m \times n$ zero matrix
J_i	= rigid body inertia along principle axis i ($i = 1, 2, 3$)
A, J, Q, R, Ω	= constant real matrices
e^A	= matrix exponential for the real matrices A
q	= unit quaternion; $\mathbf{q} = [q_1, q_2, q_3, q_4]^T := [\mathbf{q}_o^T, q_4]^T$
v_B, v	= unit vectors describing the direction of instrument's bore-sight in body and inertial coordinate frames, respectively
w_B, w	= unit vectors describing directions of a celestial object or thrust in body and inertial coordinate frames, respectively
u	= control torque
ω	= angular velocity vector
$\ x\ $	= 2-norm of vector x , i.e., $(x^T x)^{1/2}$
Diag (x)	= diagonal matrix- of appropriate dimensions- with the vector x on its diagonal
\mathcal{S}	= the unit sphere in the Euclidean space
\mathcal{S}_η	= the set of vectors with 2-norm equal to η
$\hat{\mathcal{S}}_\eta$	= the set of vectors with 2-norm greater than or equal to η
θ	= angle (in degrees)
$\alpha, \beta, \gamma, \eta, \kappa, \phi$	= constant real numbers
k, M, N	= nonnegative constants
V, Φ	= repulsive potential functions
f, g	= real-valued functions
$s(k_a, k_b)$	= sum of indexed terms starting with index k_a and ending with index k_b
$[t_0, t_f]$	= maneuver time interval
Δt	= sampling interval for time discretization
SC	= spacecraft

List of Figures

- Figure 1: A tangential exclusion path $\mathbf{q}(t_0) \rightsquigarrow \mathbf{q}(t_i) \rightsquigarrow \mathbf{q}(t_f)$ around the attitude constraint set dictated by the Sun (shaded area)
- Figure 2: Geodesic deviation between current and final attitudes for SC₁ (solid line) and SC₂ (dotted line)
- Figure 3: The inner products between inertially represented sensitive instrument vector $v(t)$ and thruster vectors $w_i(t)$ ($i = 1, 2, 3$): $v(t)^T w_1(t)$ (solid line), $v(t)^T w_2(t)$ (dotted line), and $v(t)^T w_3(t)$ (dashed line)
- Figure 4: Control torques about the x -axis exerted on SC₁ (solid line) and SC₂ (dotted line)

1 Introduction

A key software component for spacecraft operation is the guidance algorithm in charge of maneuver planning in translational and rotational degrees of freedom. The guidance algorithm, for example, is responsible for re-orienting the spacecraft- often in presence of constraints- in response to operational and scientific objectives of the mission. In this direction, consider a science space mission with the task of collecting images of distant stars and other heavenly bodies. In such a mission, the spacecraft is required to change its orientation (attitude) in some optimal manner while ensuring that its sensitive optical instruments are not exposed to very bright objects in the sky, such as the sun. An algorithmic problem that is of great practical importance is thus to determine the necessary control torques on the spacecraft such that the cones emanating from these sensitive optical devices exclude the bright object(s) during the re-orientation maneuver (Figure 1). We refer to this guidance/control problem as the spacecraft re-orientation in presence of constraints (SRPC). Different variants of SRPC appear in almost every space science mission equipped with heat or light sensitive instruments, e.g., cryogenically cooled infrared telescopes, star trackers, and low energy ion composition analyzers. A representative set of such missions includes the Cassini mission to Saturn,¹ FIRST/Planck,² and SAMPEX (Solar, Anomalous, and Magnetospheric Particle Explorer).³ In all such missions, on-board sensitive instruments are required to be protected from exposure to bright or heat generating objects. As a consequence, all reorientation and re-targeting maneuvers have to be realized via an autonomous onboard guidance law with a subroutine for addressing the SRPC.

Spacecraft re-orientation in the *absence* of constraints on permissible orientations has been extensively studied in the literature; see for example Ref. 4. On the contrary, systematic approaches to the constrained version of the problem can only be found in a handful of references despite its practical significance; these include Refs. 5-13. The SRPC can in principle be formulated as an optimal nonlinear control problem subject to nonconvex constraints. However, non-convex optimal control problems are algorithmically difficult to solve and are not attractive candidates for being embedded in an autonomous spacecraft guidance algorithm. Efficient solution strategies for the SRPC have not been available so far due to its perceived computational difficulty and possible membership in the class of NP-hard problems. In fact, the two sources of problem complexity- nonlinearity of the attitude dynamics and nonconvexity of the associated constraints- have often been considered separately. In this venue, the goal has been to solve either the nonconvex quadratically constrained control problem for linear plants (Ref. 14), or the linearly constrained control problems for the nonlinear plants (Refs. 15-17) or even the more promising linearly constrained control problems for linear plants (Refs. 18-19). Meanwhile, motivated by the new advances in the computational methods for solving convex optimization problems, a wide range of control problems have been approached via the theory convex optimization over symmetric matrices; see Ref. 20. Specifically, we note the success of this approach to resolve optimization problems with a limited number of quadratic constraints, as reported for example in Ref. 21. Our motivation in this paper is to introduce a parameterization of the spacecraft orientation in presence of constraints that can be utilized in a convex optimization framework. This on the other hand, provides a venue for embedding an

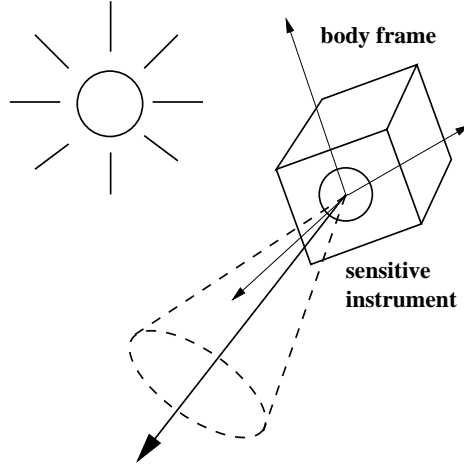


Figure 1: Sun-avoidance constraint

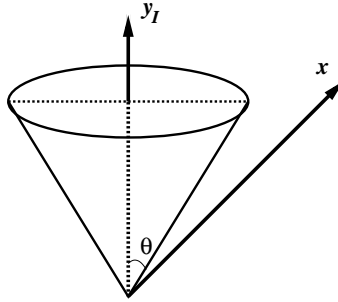


Figure 2: The exclusion zone

efficient SRPC solver in the guidance algorithm for the autonomous spacecraft operation.

1.1 Mathematical Formulation

The spacecraft re-orientation in presence of constraints can mathematically be represented as follows: given initial and terminal conditions on the angular velocity vector, $\omega(t)$, and the spacecraft attitude parameterized in terms of quaternions, $\mathbf{q}(t)$, specified by

$$\omega(t_o) = \omega_o, \mathbf{q}(t_o) = \mathbf{q}_o, \quad \text{and} \quad \omega(t_f) = \omega_f, \mathbf{q}(t_f) = \mathbf{q}_f, \quad (1)$$

with

$$\omega(t) = [\omega_1(t), \omega_2(t), \omega_3(t)]^T \in \mathbf{R}^3, \quad \mathbf{q}(t) = [q_1(t), q_2(t), q_3(t), q_4(t)]^T \in \mathbf{R}^4,$$

determine spacecraft control torques $u_i(t) \in \mathbf{R}^3$ ($i = 1, 2, 3$) over the time interval $t \in [t_0, t_f]$ subject to:

- dynamic constraints specified by Euler's equations

$$J_1 \dot{\omega}_1(t) - (J_2 - J_3) \omega_2(t) \omega_3(t) = u_1(t), \quad (2)$$

$$J_2 \dot{\omega}_2(t) - (J_3 - J_1) \omega_3(t) \omega_1(t) = u_2(t), \quad (3)$$

$$J_3 \dot{\omega}_3(t) - (J_1 - J_2) \omega_1(t) \omega_2(t) = u_3(t), \quad (4)$$

where J_i is the rigid body inertia along the principle axis i , for $i = 1, 2, 3$,

- bounded angular velocities and control torques, i.e., for given constants $\gamma_1, \gamma_2 > 0$,

$$|\omega_i(t)| \leq \gamma_1 \quad \text{and} \quad |u_i(t)| \leq \gamma_2, \quad i = 1, 2, 3, \quad (5)$$

and

- (norm preserving) kinematic constraint

$$\dot{\mathbf{q}}(t) = \frac{1}{2} \Omega(t) \mathbf{q}(t), \quad (6)$$

where

$$\Omega(t) = \begin{bmatrix} 0 & \omega_3(t) & -\omega_2(t) & \omega_1(t) \\ -\omega_3(t) & 0 & \omega_1(t) & \omega_2(t) \\ \omega_2(t) & -\omega_1(t) & 0 & \omega_3(t) \\ -\omega_1(t) & -\omega_2(t) & -\omega_3(t) & 0 \end{bmatrix},$$

guaranteeing that $\|\mathbf{q}(t)\| = 1$ for all $t \in [t_0, t_f]$.

Let us denote the set of triplet trajectories $(\mathbf{q}(t), \omega(t), u(t))$ for the rigid body re-orientation, satisfying Eqs. (1)-(6) over the time interval $[t_0, t_f]$, by \mathcal{F} , i.e.,

$$\mathcal{F} = \{(\mathbf{q}(t), \omega(t), u(t)) \mid (1) - (6) \text{ are satisfied}\}. \quad (7)$$

In this paper, in addition to the above dynamic and kinematic constraints we consider

- point-wise in time constraints on the orientation of the spacecraft represented by

$$f_i(\mathbf{q}(t)) \leq \phi_0, \quad \text{for all } t \in [t_a, t_b], \quad i = 1, 2, \dots, m, \quad (8)$$

or

$$\int_{t_a}^{t_b} g_i(\mathbf{q}(t)) dt \leq \phi_1, \quad i = 1, 2, \dots, m, \quad (9)$$

for the proper functions f_i and g_i ($i = 1, \dots, m$), constants ϕ_0, ϕ_1 , and time interval $[t_a, t_b] \subseteq [t_0, t_f]$.

Devising viable means of computationally dealing with constraints of the form (8)-(9), is one of the central themes of the present paper. More specifically, let us identify a set of constraints of the form (8)-(9) that often appear in space missions. These include:[†]

Type-I (static hard constraints): this class of constraints includes constraints imposed by celestial objects that are relatively stationary with respect to an inertial coordinate frame and those that are not actively controlled. We have in mind scenarios where there are strict non-exposure constraints on the on-board sensitive instruments with respect to celestial objects as in Refs. 1-3 and Refs. 6-10, or avoiding incoming particles, orbital debris, and micro-meteoroid fluxes as in Ref. 3. In all such settings, given unit vectors v and w in the inertial coordinate frame, describing the direction of instrument’s bore-sight and the bright celestial object, respectively, one requires that

$$v(t)^T w \leq \cos \theta \quad (10)$$

at each time instance, where θ is a required minimum angular separation; note that the angle between $v(t)$ and w is assumed to be in the range of $[0, \pi]$ without loss of generality. As we will see in §3.1, the inequality (10) translates to a constraint on the orientation of the spacecraft in the form of (8). We refer to the feasible spacecraft orientations that lead to satisfying (10) by the set \mathcal{C}_1 .

Type-II (static soft constraints): this category includes the relaxed version of Type-I constraint above. In this case, violations of the inequality (10) are allowed, however, only for a limited time interval. For instance, the cryogenically cooled telescope can be exposed to an external heat source provided that the total heat exposure does not accumulate beyond some maximally allowed level.¹³ Such constraints can be written in an integral form as

$$\int_{t_b}^{t_a} |v(t)^T w| dt \leq \phi_1, \quad (11)$$

where $[t_a, t_b] \subseteq [t_0, t_f]$ is the maneuver time interval during which we allow the constraint violation $v(t)^T w > \cos \theta$, ϕ_1 is a fixed constant (that depends on exposure time limitations), and the angle between $v(t)$ and w is assumed to be in the range of $[0, \pi]$. As we will see in § 4.1, the inequality (11) translates to an inequality constraint on the orientation of the spacecraft. We refer to the feasible spacecraft orientations that lead to satisfying (11) by the set \mathcal{C}_2 .

Type-III (dynamic constraints)[‡]: these constraints have rarely been considered in past but they are of great importance in the context of multiple spacecraft formation flying. Type-III constraints encompass scenarios where the plume generated by firing a particular thruster on

[†]As identified by the authors after an extensive literature search.

[‡]We include dynamic “hard” constraints in this section; nevertheless, dynamic “soft” constraints can be addressed in a similar fashion.

one spacecraft results in damaging the sensitive instruments mounted on another spacecraft. Note that in this case, the source of attitude constraints are themselves dynamic and often actively controlled; in fact, they can be represented by the inequality

$$v(t)^T w(t) \leq \cos \theta, \quad (12)$$

with the standing assumption that the angle between the two vectors remain in the range of $[0, \pi]$. As we will see in § 4.2, the inequality (12) translates to an inequality constraint on the orientation of the spacecraft. We refer to the feasible spacecraft orientations that lead to satisfying (12) by the set \mathcal{C}_3 .

Type-IV (mixed constraints): in this last category, we include various possible combinations of the preceding three types of constraints. Most space science missions, particularly those involving multiple spacecraft formation flying, have mixed attitude constraints. Evidently, the presence of mixed constraints further complicates the required attitude maneuver planning and trajectory design for these missions.

Definition 1.1 *The re-orientation of a rigid spacecraft in presence of constraints is the problem of finding the triplet trajectories $(\mathbf{q}(t), w(t), u(t))$ at the intersection*

$$\mathcal{F} \cap \mathcal{C}$$

where \mathcal{F} is defined as in (7) and \mathcal{C} denotes the intersection of \mathcal{C}_1 , \mathcal{C}_2 and/or \mathcal{C}_3 as dictated by the class of orientation constraints imposed on the spacecraft.

In this paper, after reviewing several approaches to the constrained spacecraft re-orientation problem, we proceed to discuss an approach- based on convex optimization- that promises a wide applicability as well as computational efficiency for autonomous spacecraft guidance. The organization of the paper is as follows. An overview of existing methods for solving the SRPC, including those relying on geometric constructions, artificial potential functions, constraint monitoring, randomized motion planning, and finally semidefinite programming, is provided in §2. In §3-5, we present a convex approach to the general class of SRPC problems. §5 concludes the paper with an example demonstrating the viability of the proposed framework in a multiple spacecraft setting.

2 Existing Frameworks

In this section we provide an overview of the existing frameworks for solving the SRPC problem for various classes of constraints.

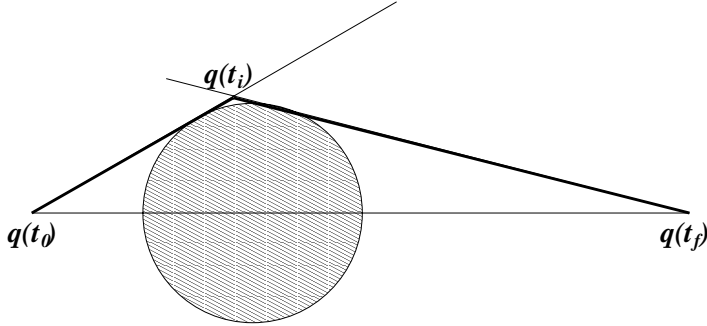


Figure 3: A tangential exclusion path $\mathbf{q}(t_0) \rightsquigarrow \mathbf{q}(t_i) \rightsquigarrow \mathbf{q}(t_f)$ around the attitude constraint set dictated by the Sun (shaded area)

2.1 Geometric Algorithms

The geometric approach, as exemplified in Refs. 6 – 7, relies on geometric relations between vectors v and w in (10) to handle constraints of Types I. The main ingredient of this framework is determining a feasible attitude trajectory prior to initiating the reconfiguration, if possible, or finding feasible attitudes whenever an avoidance maneuver is needed during the course of the attitude slew (see Refs. 3 and 13). Generally in this venue an optimal or an easily implementable on-board control for the unconstrained attitude maneuver between two arbitrary orientations is first considered. Then, the algorithm seeks an intermediate attitude $q(t_i)$ (a way-point) between $q(t_0)$ and $q(t_f)$, such that the aforementioned control strategy- without any constraint violation- can be applied for each time interval $[t_0, t_i]$ and $[t_i, t_f]$. A typical example for such an approach- as found in Ref. 6- involves finding a tangential exclusion path,

$$\mathbf{q}(t_0) \rightsquigarrow \mathbf{q}(t_i) \rightsquigarrow \mathbf{q}(t_f),$$

such that the unconstrained maneuver planning for each subdivision can easily be accomplished (Fig. 3). Another explicit way to determine feasible intermediate attitudes for Type-I constraints is provided in Ref. 7. We note that although the geometric approach enjoys a certain level of conceptual simplicity, it is mainly applicable to problems where only a small number of constraints are present and selection of the attitude way-points is computationally feasible and/or relatively straightforward.

2.2 Potential Function-based Algorithms

Potential functions have been recognized as one of the main tools for handling kinematic constraints that arise not only in the SRPC problem, but more generally, in a wide array of problems in robotics and related fields. The starting point for this approach as it pertains to the SRPC problem,

is constructing one or multiple outward vectors with respect to the constraints. Subsequently, one proceeds to linearly combine these vectors, with appropriate weights, to generate a “repellent” control torque with respect to the constrained set. For example in Ref. 8, the repulsive potential $V_{\alpha,\beta}$ is first defined by

$$V_{\alpha,\beta}(\theta) = \sum_{j=1}^m \Phi_j(\theta), \quad (13)$$

where

$$\Phi(\theta) = \alpha e^{-\beta \sum_{i=1}^3 (\theta_i - \hat{\theta}_i)^2},$$

with

$$\dot{\theta}_i(t) = \sum_{j=1}^3 \begin{bmatrix} 1 & \sin \theta_1(t) \tan \theta_2(t) & \cos \theta_1(t) \tan \theta_2(t) \\ 0 & \cos \theta_1(t) & -\sin \theta_1(t) \\ 0 & \sin \theta_1(t) \sec \theta_2(t) & \cos \theta_1(t) \sec \theta_2(t), \end{bmatrix} \omega_j(t),$$

θ is the Euler angle, $\hat{\theta}$ is the attitude angle associated with Type-I constraint (10), parameters α and β shape the potential function, and m is the number of constraints. The potential $V_{\alpha,\beta}$ (13) is then combined with functions constructed for other purposes (e.g., to minimize the maneuver time); the combination of these functions is then optimized at each time instance to obtain slew maneuvers for the required attitude reconfiguration. An analogous approach for obtaining constraint avoidance forces can be found in Ref. 7. Parallel to the same line of reasoning, an interesting direction that has been pursued in the potential function framework proceeds to characterize the set Γ of forbidden attitude quaternions via two orthonormal vectors z_1 and z_2 . The vectors z_1, z_2 are then utilized in defining the repulsive potential as

$$V_k(\mathbf{q}) = \frac{k(1 - q_4)}{(\mathbf{q}^T z_1)^2 + (\mathbf{q}^T z_2)^2}, \quad (14)$$

where k is chosen as a positive constant.⁹ Now since

$$\mathbf{q} \text{ violates the constraints if } (\mathbf{q}^T z_1)^2 + (\mathbf{q}^T z_2)^2 = 0,$$

one expects that the repulsive control defined as

$$u_k(\mathbf{q}) = -\frac{\partial V_k(\mathbf{q})}{\partial \mathbf{q}},$$

yields the torque required for the constrained reorientation. One of the main draw backs of this approach is that convergence to the target attitude can not be guaranteed. This is in light of the fact that

superposition of potential functions of the form (14) often leads to functionals that are nonconvex.[†] Moreover, the existence of vectors z_1 and z_2 above, utilized to characterize the constraint set, is not ensured- particularly as the number of Type-I constraints increases. The potential function-based algorithms do not generally guarantee the satisfaction of Type-I constraints, and hence, one might in fact end up with a slight violation of critical constraints. Moreover, there is no guarantee that the resulting path will satisfy rate and torque constraints which are often of importance in practice.

2.3 Constraint Monitor Algorithms

The constraint monitor algorithm (CMT) as described in Refs. 1 and 10, is a real-time algorithm which actively monitors the constraints of all types and prescribes required avoidance actions. The algorithm designed originally for the Cassini mission to Saturn has also flown successfully on the Deep-Space 1 mission.¹⁴ In the constraint monitor architecture, a compliant path is not computed a-priori; rather, a feasible path is computed in real-time by using a predictor-corrector approach. In this venue, the current attitude motions are projected forward (local and short-duration) and corrective actions are taken when the predicted motion is found to be non-compliant. The algorithm, although sub-optimal, can be executed in real-time, and is eminently suited to the Cassini attitude and articulation control system architecture. The CMT architecture also guarantees that prescribed paths do not violate any of the required rate and acceleration limitations imposed on attitude motions. In the meantime, the issue of convergence for the constraint monitor algorithm can only be addressed in a case-by-case basis. Generally, one needs to resort to extensive mission simulations to demonstrate the viability of the algorithm.

2.4 Randomized Algorithms

Randomized motion planning algorithms have been used to solve the constrained attitude problem in Refs. 11 and 12. These algorithms are based on following ingredients: (1) initialize a graph G_0 consisting of a distinct vertex v_0 representing initial states $\mathbf{q}(t_0), \omega(t_0)$, (2) at iteration $k + 1$, perform a random search, starting from v_k , to determine a set of feasible vertices among the vertices of graph G_k , (3) select a feasible vertex, among those found in (2) such that a given cost functional is minimized; call this vertex v_{k+1} , (4) repeat steps (2)-(3), now initiated from v_{k+1} ; replace the index k with $k + 1$. Iterate until the final attitude $\mathbf{q}(t_f)$ is achieved, and (5) apply an optimal control torque for each attitude trajectory subdivision found.

The random search approach has the advantage that it can deal with all types of trajectory constraints. However, one of its potential drawbacks is that convergence to the final attitude can be guaranteed only in a probabilistic sense: it can be shown that as the number of vertices in the state

[†]In Ref. 8, it is stated that the proposed approach applied to a single Type-I constraint has a guaranteed convergence behavior.

graph increases, the probability of an incorrect termination exponentially decays to zero. Meanwhile, we note that the computational effort in searching for a feasible node at each time step increases dramatically as the size of the underlying graph grows.

2.5 Semidefinite Programming-based Algorithms

We conclude our overview by mentioning the recently proposed semidefinite programming (SDP) approach to constrained attitude control.⁵ This approach will be shortly elaborated upon, as it provides the main theme for the present paper. The SDP approach essentially exploits the nonlinearity of dynamics and kinematic constraints on one hand, and the structured nonconvexity of attitude constraints on the other, to propose a convexified SDP formulation of the original SRPC problem. An SDP is the optimization problem involving a linear objective functional and a constrained set defined by linear matrix inequalities (LMIs).²⁰ An LMI on the other hand, is an inequality over matrix variables, interpreted with respect to the positive semidefinite ordering (see the Nomenclature section). The advantage of such an SDP formulation of the SRPC problem is its solvability via the available efficient convex optimization software, e.g., Ref. 23.

3 Convex Approach to Constrained Re-orientation

In this section we delve into the convex parametrization of Type I constraints on the spacecraft re-orientation. Our primary goal is to demonstrate that- although the set represented by this class of constraints is generally nonconvex- an intrinsic property of the attitude parametrization via quaternions can be utilized to convexify the corresponding constraint set. This on the other hand, opens up an efficient avenue for solving constrained spacecraft re-orientation problems via convex optimization algorithms.

3.1 Type-I Constraints

The convex approach to the SRPC with Type-I constraints is based on the observation that the corresponding set of admissible quaternions can be parameterized via quadratic inequalities.^{1,10} Recall that during the attitude maneuver, this class of constraints requires that

$$v(t)^T w \leq \cos \theta, \quad (15)$$

at each time instance, where the unit inertial vectors v and w , denote, respectively, the instrument's bore-sight and the bright, relatively stationary, celestial object; θ is a minimum angular separation allowed between $v(t)$ and w during the attitude slew and is assumed to be in the range of $[0, \pi]$; see Figs. 1 and 2. We now employ the coordinate transformation formula, relating inertial and body vectors via the quaternion representation of spacecraft attitude by²⁴

$$v(t) = v_B - 2(\mathbf{q}_o^T \mathbf{q}_o) v_B + 2(\mathbf{q}_o^T v_B) \mathbf{q}_o + 2q_4 (v_B \times \mathbf{q}_o); \quad (16)$$

in (16) we have adopted the notation

$$\mathbf{q}_o := [q_1, q_2, q_3]^T,$$

and v_B represents the inertial vector v in body coordinates. Combining (15) and (16), followed by a few algebraic operations, we are led to the equivalent quaternion characterization of the constrained set in terms of the quadratic inequality

$$\mathbf{q}(t)^T \tilde{A} \mathbf{q}(t) \leq 0, \quad (17)$$

with

$$\tilde{A} := \tilde{A}(v_B, w, \theta) = \begin{bmatrix} A & b \\ b^T & d \end{bmatrix} \in \mathbf{R}^{4 \times 4}, \quad (18)$$

and

$$\begin{aligned} A &:= v_B w^T + w v_B^T - (v_B^T w + \cos \theta) I_3, \\ b &:= w \times v_B, \quad d_i := v_B^T w - \cos \theta; \end{aligned}$$

this derivation parallels the analogous discussion in Ref. 1. Note that the matrix \tilde{A} in (17) is symmetric and therefore has a real set of eigenvalues. In this meantime, since \tilde{A} is not positive semidefinite, the set defined by inequality (17) is nonconvex in the spacecraft orientation represented by $\mathbf{q}(t)$.

As finding a feasible point in a nonconvex set is computationally difficult in general, in Ref. 5, we proposed an alternative parametrization of (17) in terms of a convex quadratic inequality or a linear matrix inequality. The proposed approach relies on the following proposition.

Proposition 3.1 *Given an $n \times n$ symmetric matrix A , assume that the set*

$$\mathcal{A} := \{\mathbf{q} \in \mathbf{R}^n \mid \mathbf{q}^T A \mathbf{q} \leq 0\}, \quad (19)$$

has a nonempty intersection with the unit sphere \mathcal{S} . Suppose that \mathbf{q} is priori known to belong to \mathcal{S} . Then \mathbf{q} is feasible for \mathcal{A} (19) if and only if it is feasible for the convex set defined by

$$\mathbf{q}^T (A + \mu I) \mathbf{q} \leq \mu, \quad (20)$$

where $A + \mu I$ is positive definite, e.g., μ is larger than the minimum eigenvalue of A .

Proof: Since

$$\mathbf{q}^T (A + \mu I) \mathbf{q} = \mathbf{q}^T A \mathbf{q} + \mu \mathbf{q}^T \mathbf{q} = \mathbf{q}^T A \mathbf{q} + \mu$$

the equivalence follows. We note that when μ is larger than the minimum eigenvalue of A , the sum $A + \mu I$ is positive definite and hence, the set defined by (20) is convex. ■

Proposition 3.1 states that although the set \mathcal{A} (19) is not convex for an indefinite matrix A , it admits a convex parametrization (20) when it is considered in the relative topology induced by the unit sphere. In fact, one convenient parameterization of the resulting convex set is in terms of linear matrix inequalities. This is facilitated through the Schur complement formula, stating that when A is positive definite (which will be denoted as $A > 0$), one has

$$\begin{bmatrix} A & B \\ B^T & C \end{bmatrix} > 0 \quad \text{if and only if} \quad C - B^T A^{-1} B > 0; \quad (21)$$

see Ref. 15. Using the Schur complement relation (21), Proposition 3.1 can be generalized in several different ways, including the following two observations (see Ref. 5).

Proposition 3.2 *Let A_i 's be a set of symmetric matrices and b_i 's be a set of real numbers ($i = 1, 2, \dots, m$). Then the set*

$$\{\mathbf{q} \in \mathbf{R}^n \mid \mathbf{q}^T A_i \mathbf{q} \geq b_i, i = 1, 2, \dots, m\}, \quad (22)$$

intersected with a sphere of radius η (denoted by \mathcal{S}_η) can be represented by the the linear matrix inequalities

$$\begin{bmatrix} \mu_i \eta^2 - b_i & x^T \\ x & \tilde{A}_i \end{bmatrix} \geq 0, \quad i = 1, \dots, m, \quad (23)$$

where

$$\tilde{A}_i := (\mu_i I_n - A_i)^{-1},$$

and for each i , μ_i is strictly greater than the largest eigenvalue of A_i (and hence \tilde{A}_i and its inverse are positive definite).

In Proposition 3.2, the requirement that \mathbf{q} is priori known to belong to the sphere of radius η can be relaxed in the following way.

Proposition 3.3 *Let*

$$\hat{\mathcal{S}}_\eta := \{\mathbf{q} \in \mathbf{R}^n \mid \|\mathbf{q}\| \geq \eta\}. \quad (24)$$

Then $\mathbf{q} \in \hat{\mathcal{S}}_\eta$ satisfying the matrix inequalities (23) is an element of the set (22).

Propositions 3.1 is utilized in the context of constrained attitude guidance in the following way. Since the spacecraft attitude has been parameterized in terms of quaternions, and the quaternion trajectory $\mathbf{q}(t)$ *implicitly* evolves on the unit sphere \mathcal{S} , Propositions 3.1 can be employed to conclude that the spacecraft guidance problem in presence of an *arbitrary* number of nonconvex Type-I constraints, can be parameterized as a convex set defined by linear matrix inequalities. In particular,

this observation would completely solve the SRPC if one could seamlessly augment the nonlinear dynamic equations (2)-(4) to this convex program. However, as augmenting the nonlinear differential equality constraint destroys the convexity of the corresponding feasible set, one needs to resort to a linear approximation of the dynamic equations.¹

3.2 Computational Ramifications of the Convex Approach to the SRPC

Let us consider the ramification of the convex parameterization of Type I constraints in terms of solving the autonomous SRPC problem. One simple first order scheme to approximate the Euler's equations is as follows: we consider the discretization of Eqs. (2)-(4) and with a proper sampling time Δt as,

$$\Delta t \dot{\omega}(t) \approx \omega(k+1) - \omega(k)$$

and propagate the orientation of the spacecraft over the time interval Δt as

$$\mathbf{q}(k+1) = e^{\frac{\Delta t}{2}\Omega(k)}\mathbf{q}(k) \quad (25)$$

where

$$\Omega(k) := \begin{bmatrix} 0 & \omega_3(k) & -\omega_2(k) & \omega_1(k) \\ -\omega_3(k) & 0 & \omega_1(k) & \omega_2(k) \\ \omega_2(k) & -\omega_1(k) & 0 & \omega_3(k) \\ -\omega_1(k) & -\omega_2(k) & -\omega_3(k) & 0 \end{bmatrix}.$$

Using this scheme, the convex optimization approach to constrained attitude guidance with Type-I constraints assumes the following form: we iteratively solve the convex optimization problem (26)-(32) for $k = 0, 1, \dots, N-1$:

$$\min_{x(k)} \alpha \quad (26)$$

subject to

$$\text{parameterizing (8): } x(k)^T \{H^T \tilde{A}_i H\} x(k) \leq 0, \quad i = 1, 2, \dots, m, \quad (27)$$

or as a convex linear matrix inequality

$$\text{parameterizing (8): } \begin{bmatrix} \mu_i & (Hx(k))^T \\ Hx(k) & (\mu_i I_4 + \tilde{A}_i)^{-1} \end{bmatrix} \geq 0, \quad i = 1, 2, \dots, m, \quad (28)$$

¹We note that such an approximation is not needed for a symmetric spacecraft or if one utilizes a feedback linearization scheme.

$$\text{parameterizing (1):} \quad \begin{bmatrix} \alpha & (E(k)^{1/2} \begin{bmatrix} x(k) \\ 1 \end{bmatrix})^T \\ E(k)^{1/2} \begin{bmatrix} x(k) \\ 1 \end{bmatrix} & I_{11} \end{bmatrix} \geq 0, \quad (29)$$

$$\text{parameterizing (2)-(4) \& (6):} \quad F(k)x(k) = y(k), \quad (30)$$

$$\text{parameterizing (5):} \quad |G_1 x(k)| \leq \gamma_1 [1 \ 1 \ 1]^T, \quad (31)$$

$$\text{parameterizing (5):} \quad |G_2 x(k)| \leq \gamma_2 [1 \ 1 \ 1]^T, \quad (32)$$

where $E(k) \in \mathbf{S}_+^{11}$, $F(k) \in \mathbf{R}^{7 \times 10}$, $G_1, G_2 \in \mathbf{R}^{10 \times 10}$, and $H \in \mathbf{R}^{4 \times 10}$. In Eqs. (28)-(32) we have

$$E(k) = \begin{bmatrix} 0_{3 \times 3} & 0_{3 \times 3} & 0_{3 \times 4} & 0_{3 \times 1} \\ 0_{3 \times 3} & I_3 & 0_{3 \times 4} & \omega(N) \\ 0_{4 \times 3} & 0_{4 \times 3} & 0_{4 \times 4} & 0_{4 \times 1} \\ 0_{1 \times 3} & \omega(N)^T & 0_{1 \times 4} & \omega(N)^T \omega(N) \end{bmatrix} + \begin{bmatrix} 0_{6 \times 6} & 0_{6 \times 4} & 0_{6 \times 1} \\ 0_{4 \times 6} & Q(N)^T Q(N) & 0_{4 \times 1} \\ 0_{1 \times 6} & 0_{1 \times 4} & 0_{1 \times 1} \end{bmatrix},$$

$$F(k) = \left[\begin{array}{c|c|c} -\Delta t I_3 & J & 0_{4 \times 4} \\ \hline 0_{4 \times 3} & 0_{4 \times 3} & e^{-R(k)} \end{array} \right],$$

where

$$J := \begin{bmatrix} J_1 & 0 & 0 \\ 0 & J_2 & 0 \\ 0 & 0 & J_3 \end{bmatrix}, \quad R(k) := \frac{\Delta t}{2} \begin{bmatrix} 0 & \omega_3(k) & -\omega_2(k) & \omega_1(k) \\ -\omega_3(k) & 0 & \omega_1(k) & \omega_2(k) \\ \omega_2(k) & -\omega_1(k) & 0 & \omega_3(k) \\ -\omega_1(k) & -\omega_2(k) & -\omega_3(k) & 0 \end{bmatrix}$$

$$G_1 := \begin{bmatrix} 0_{3 \times 3} & I_3 & 0_{3 \times 4} \end{bmatrix}, \quad G_2 := \begin{bmatrix} I_3 & 0_{3 \times 7} \end{bmatrix},$$

$$x(k) := \begin{bmatrix} u_1(k) \\ u_2(k) \\ u_3(k) \\ w(k+1) \\ \mathbf{q}(k+1) \end{bmatrix}, \quad y(k) := \begin{bmatrix} J_1 w_1(k) + \Delta t (J_2 - J_3) \omega_2(k) \omega_3(k) \\ J_2 w_2(k) + \Delta t (J_3 - J_1) \omega_3(k) \omega_1(k) \\ J_3 w_3(k) + \Delta t (J_1 - J_2) \omega_1(k) \omega_2(k) \\ \mathbf{q}(k) \end{bmatrix},$$

$$H = \begin{bmatrix} 0_{4 \times 6} & I_{4 \times 4} \end{bmatrix}, \quad Q(N) := \begin{bmatrix} q_4(N) & q_3(N) & -q_2(N) & -q_1(N) \\ -q_3(N) & q_4(N) & q_1(N) & -q_2(N) \\ q_2(N) & -q_1(N) & q_4(N) & -q_3(N) \\ q_1(N) & q_2(N) & q_3(N) & q_4(N) \end{bmatrix},$$

μ_i is chosen to be strictly greater than the largest eigenvalue of $-\tilde{A}_i$; the matrix \tilde{A}_i is as defined in (18). In such a setup, the convex program (26)-(32) is solved for $x(k)$, $k = 0, 1, \dots, N - 1$, where $(\Delta t)N$ is the time interval $[t_0, t_f]$ as designated for the required reorientation. The role of the parameter α in (26) and (29) is to steer the spacecraft toward the desired terminal orientation $\mathbf{q}(N)$ and angular velocity $\omega(N)$. Under the assumption that for each k this problem is feasible, the approach offers convergence guarantee to the final desired spacecraft orientation. Note that due to the propagation scheme (25), the quaternion updates always remain on the unit sphere. The program (26)-(32) can be augmented with a similar set of inequality and equality constraints on future states $x(k+1)$, $x(k+2)$, etc.² This might be desired to ensure constraint avoidance in a look-ahead type of algorithm over a finite time horizon. We also note that other computational techniques for accurate quaternion updates are available (see Ref. 1), which can be used in conjunction with the proposed convex optimization approach.

4 Type-II through Type IV Constraints

Let us now extend the convex optimization framework proposed in §3 to other classes of constraints on the orientation of the spacecraft. In view of the problem formulation (26)-(32), it is evident that this can be achieved via a convex parameterization of other classes constraints analogous to (27) or (28). At that point, one only needs to replace (27) or (28) with the derived inequality constraints and obtain a convex optimization problem for the corresponding instance of SRPC.

4.1 Type-II Constraints

Let us consider Type-II constraints of the form

$$\int_{t_a}^{t_b} v(t)^T w dt \leq \phi_1, \quad (33)$$

or in its discretized form

$$s(k_a, k_b) := \sum_{k=k_a}^{k_b} v(k)^T w \leq \phi_1, \quad (34)$$

²Via a linear approximation of the matrix exponential in (25) or assuming that the angular velocity has not significantly changed from the previous time step.

where $[t_a, t_b] \subseteq [t_0, t_f]$ is the maneuver time interval during which we allow the constraint violation $v(t)^T w > \cos \theta$. In our discussion of this class of constraints, we will implicitly assume that the desired minimum angular separation satisfies $\theta \in [0, \pi/2]$; however, the case of $\theta \in [\pi/2, \pi]$ can be handled in the similar manner. As the convex approach of §3 is inherently an iterative algorithm, let us consider its suitable extension allowing us to address constraints of the form of Eq. (34). Our approach proceeds as follows:

1. if there are no constraint violations, solve the problem (26)-(32) without including the constraint (28).
2. if the attitude constraint (17) is not satisfied at the k_a -th step and the estimated sum $\tilde{s}(k_a, k_b)^\dagger$ is less than ϕ_1 , proceed with Step 1. Otherwise, solve the convex optimization (35)-(36) to escape the attitude exclusive zone:

$$\min_{x(k)} \alpha + M\beta \quad (35)$$

subject to

$$x(k)^T \{H^T \tilde{A}_i H\} x(k) \leq \beta, \quad i = 1, 2, \dots, m,$$

or equivalently the LMIs

$$\begin{bmatrix} \mu_i + \beta & (Hx(k))^T \\ Hx(k) & (\mu_i I_4 + \tilde{A}_i)^{-1} \end{bmatrix} \geq 0, \quad i = 1, 2, \dots, m \quad (36)$$

in conjunction with Eq. (29)-(32), with M chosen as a large positive constant.

A moment reflection on the inclusion of parameter M in the objective functional (35) reveals that this modified objective ensures that the algorithm guides the spacecraft orientation to exit the constrained region as quickly as possible.³ This on the other hand leads to an attitude maneuver that respects the integral constraint (33) that characterizes Type-II constraints.

4.2 Type-III Constraints

As it was pointed out in §II, Type-III constraints often arise in the context of multiple spacecraft formation flying. In this venue, consider a dual-spacecraft system and let v and w be specified in each spacecraft body frame. Let us recall that Type-III constraints assume the form

$$v(t)^T w(t) \leq \cos \theta, \quad (37)$$

[†]One way to estimate $s(k_a, k_b)$ is by directly integrating Eqs. (2)-(4) and (6) with a pseudo control force.

³The exit time depends on the magnitude of the weight M in (35).

where both vectors v and w are time-varying and controlled. In view of the coordinate transformation in Eq. (16), we realize that Eq. (37) is no longer quadratic in the corresponding attitude quaternions q^v and q^w , as

$$\begin{aligned} v(t) &= v_B - 2(q_o^v(t)^T q_o^v(t)) v_B + 2(q_o^v(t)^T v_B) q_o^v(t) \\ &\quad + 2q_4^v(t) (v_B \times q_o^v(t)) \end{aligned} \quad (38)$$

$$\begin{aligned} w(t) &= w_B - 2(q_o^w(t)^T q_o^w(t)) w_B + 2(q_o^w(t)^T w_B) q_o^w(t) \\ &\quad + 2q_4^w(t) (w_B \times q_o^w(t)). \end{aligned} \quad (39)$$

Nevertheless, let us make a few observations that will make the convex optimization formulation of §3 a viable approach to handle this more complex scenario. First recall that attitude constraints of Type-III are of the form

$$\begin{bmatrix} v(t) \\ w(t) \end{bmatrix}^T \begin{bmatrix} 0_{3 \times 3} & I_3 \\ I_3 & 0_{3 \times 3} \end{bmatrix} \begin{bmatrix} v(t) \\ w(t) \end{bmatrix} \leq 2 \cos \theta. \quad (40)$$

In the case where the quaternions are accurately updated, i.e., when both q^v, q^w are priori on the unit sphere \mathcal{S} , one has,

$$\left\| \begin{bmatrix} v(t) \\ w(t) \end{bmatrix} \right\| = (\|v(t)\|^2 + \|w(t)\|^2)^{\frac{1}{2}} = \sqrt{2}.$$

Thus

$$[v(t)^T \ w(t)^T]^T \in \mathcal{S}_{\sqrt{2}},$$

and in view of Proposition 3.1, Eq. (40) can be convexified via the Schur complement formula (21) as

$$\begin{bmatrix} 2(\mu + \cos \theta) & \begin{bmatrix} v(t) \\ w(t) \end{bmatrix}^T \\ \begin{bmatrix} v(t) \\ w(t) \end{bmatrix} & D \end{bmatrix} \geq 0, \quad (41)$$

where μ is chosen such that

$$D := (\mu I_6 + \begin{bmatrix} 0_{3 \times 3} & I_3 \\ I_3 & 0_{3 \times 3} \end{bmatrix})^{-1} \quad (42)$$

is positive definite. In order to include (38)-(39) in our optimization framework, specifying the relation between vectors represented in inertial and body coordinate frames, an additional six quadratic

inequalities are augmented to our original convex optimization formulation. For example, for the first coordinate of $v(t)$, denoted by $v_1(t)$, one can write

$$q^v(t)^T C_1^v q^v(t) = v_1(t) - (v_B)_1, \quad (43)$$

where

$$C_1^v = \begin{bmatrix} 0 & (v_B)_2 & (v_B)_3 & 0 \\ (v_B)_2 & -2(v_B)_1 & 0 & -(v_B)_3 \\ (v_B)_3 & 0 & -2(v_B)_1 & (v_B)_2 \\ 0 & -(v_B)_3 & (v_B)_2 & 0 \end{bmatrix}$$

and $v_B = [(v_B)_1, (v_B)_2, (v_B)_3]^T$. The equality (43), on the other hand, can be represented by two quadratic inequalities,

$$q^v(t)^T C_1^v q^v(t) \geq v_1(t) - (v_B)_1, \quad (44)$$

and

$$q^v(t)^T C_1^v q^v(t) \leq v_1(t) - (v_B)_1. \quad (45)$$

Now Proposition 3.1 can be applied to (44)-(45) in order to convexify these inequalities by representing them as linear matrix inequalities

$$L_{1+}^v(t) := \begin{bmatrix} \mu_1 - v_1(t) + (v_1)_B & q^v(t)^T \\ q^v(t) & (\mu_1 I_4 - C_1^v)^{-1} \end{bmatrix} \geq 0$$

and

$$L_{1-}^v(t) := \begin{bmatrix} \mu_2 + v_1(t) - (v_1)_B & q^v(t)^T \\ q^v(t) & (\mu_2 I_4 + C_1^v)^{-1} \end{bmatrix} \geq 0,$$

where μ_1 and μ_2 are strictly greater than the largest eigenvalues of C_1^v and $-C_1^v$ in (44)-(45), respectively. Thus, our convex optimization formulation of the SRPC with Type-III constraints, involves iterations of the form

$$\min_{x^v(k), x^w(k), v(k+2), w(k+2)} \alpha^v + \alpha^w$$

subject to

$$\begin{bmatrix} 2(\mu + \cos \theta) & \begin{bmatrix} v(k+2) \\ w(k+2) \end{bmatrix}^T \\ \begin{bmatrix} v(k+2) \\ w(k+2) \end{bmatrix} & D \end{bmatrix} \geq 0,$$

approach	Type-I	Type-II	Type-III	Type-IV
geometric	✓	–	–	–
potential function	✓	–	–	–
constraint monitoring	✓	✓	✓	✓
randomized	✓	✓	✓	✓
convex optimization	✓	✓	✓	✓

Table 1: Applicability and convergence properties of the various frameworks for solving the SRPC problem.

$$L_{j+}^v(k+2) \geq 0, \quad L_{j-}^v(k+2) \geq 0, \quad L_{j+}^w(k+2) \geq 0, \quad L_{j-}^w(k+2) \geq 0,$$

where D is defined by Eq. (42) and $j \in \{1, 2, 3\}$, in conjunction with constraints (29)-(32) associated with variables $x^v(k)$ and $x^w(k)$.

4.3 Type-IV Constraints

The most convenient feature of the convex programming approach to SRPC is its ability to handle various *combinations* of all foregoing types of constraints. In this venue, we notice that all these constraints can accurately be represented by convex quadratic inequalities or linear matrix inequalities. Such a representation, on the other hand, leads to a convex programming solution to a wide array of SRPC problems augmented with mixed constraints. Table 1 summarizes the applicability of the various algorithmic frameworks for solving the SRPC problem as considered in this paper.

5 An example

In this section, we present an example for solving a SRPC problem subject to multiple Type-III constraints via the proposed approach. As mentioned in §4.2 multiple spacecraft formation flying missions are of the main source of this class of problems. Specifically, we consider the problem of constrained relative attitude control in a dual-spacecraft mission; the two spacecraft are assumed to be in close proximity of each other. The dual-spacecraft, denoted by SC_1 and SC_2 , respectively, have thrusters capable of providing control torques aligned with each principal axes; SC_1 is assumed to have an on-board sensitive instrument. Our objective is to find a sequence of control torques $u(k)$ ($k = 0, 1, 2, \dots$), such that SC_1 and SC_2 change their orientations from initial states $(q_1(t_0), \omega_1(t_0))$ and $(q_2(t_0), \omega_2(t_0))$, to final states $(q_1(t_f), \omega_1(t_f))$ and $(q_2(t_f), \omega_2(t_f))$, while the sensitive instrument on-board SC_1 is not in a constrained cone around particular thrust directions

emanating from SC_2 during the entire attitude slew. The physical constants and the initial and terminal conditions for our example are as follows: principle axes of inertia are

$$\mathbf{Diag} [J_1, J_2, J_3] = \mathbf{Diag} [100, 200, 300] \text{ kg m}^2,$$

initial angular velocities,

$$\omega_1(t_0) = \omega_2(t_0) = [0, 0, 0]^T \text{ rad/sec},$$

final angular velocities,

$$\omega_1(t_f) = \omega_2(t_f) = [0, 0, 0]^T \text{ rad/sec},$$

initial attitude quaternions,

$$\begin{aligned} q_1(t_0) &= [0.0000, 0.0000, 0.0000, 1.0000]^T, \\ q_2(t_0) &= [-0.5000, 0.5000, 0.5000, 0.5000]^T, \end{aligned}$$

final attitude quaternions,

$$\begin{aligned} q_1(t_f) &= [-0.5000, 0.5000, 0.5000, 0.5000]^T, \\ q_2(t_f) &= [0.0000, 0.0000, 0.0000, 1.0000]^T, \end{aligned}$$

the sensitive instrument vector in the body frame attached to SC_1 is,

$$v_B = [0.750, 0.433, 0.500]^T,$$

the thruster vectors in the body coordinate frame attached to SC_2 are,

$$(w_1)_B = [1, 0, 0]^T, \quad (w_2)_B = [0, 1, 0]^T, \quad (w_3)_B = [0, 0, 1]^T,$$

and finally, the required angular separation is required to be $\theta = 50$ deg. The initial and the desired final attitude quaternions have been chosen to satisfy (37), i.e., the sensitive instrument on SC_1 is outside the three constraint cones emanating from the bore-sight of each thruster on SC_2 , or more precisely,

$$\begin{aligned} v(t_0)^T w_1(t_0) &\leq \cos \theta (= 0.6428), \\ v(t_0)^T w_2(t_0) &\leq \cos \theta, \\ v(t_0)^T w_3(t_0) &\leq \cos \theta, \end{aligned}$$

where v and w_1, w_2, w_3 are the inertially represented vectors corresponding to u_B and $(w_1)_B, (w_2)_B,$ and $(w_3)_B$, respectively. Figure 4 depicts the geodesic distance to the final attitudes for SC_1 (solid line) and SC_2 (dotted line) under the guidance of the convex-optimization based reconfiguration algorithm. In Figure 5, each line represents the value of $v(t)^T w_i(t)$ for $i = 1$ (solid line), 2 (dotted line), and 3 (dashed line). As seen in this figure, the constraints $v(t)^T w_2(t) \leq \cos \theta$

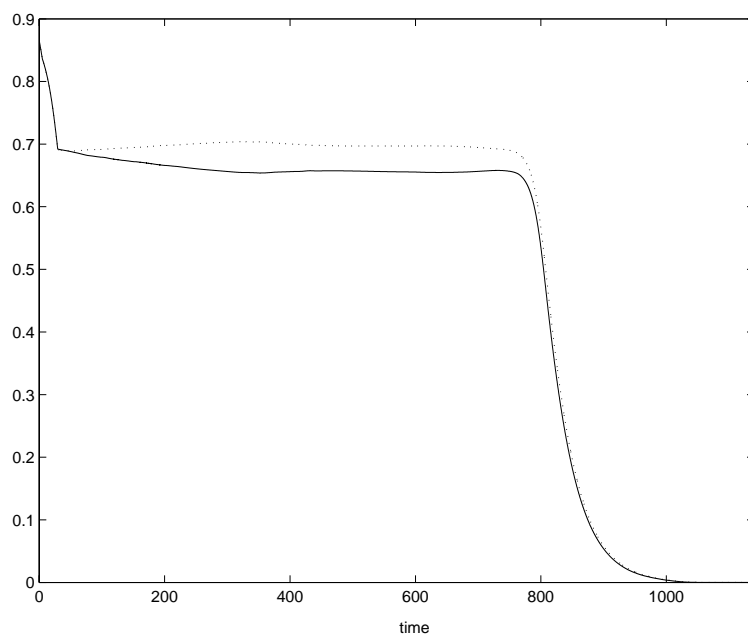


Figure 4: Geodesic deviation between current and final attitudes for SC₁ (solid line) and SC₂ (dotted line).

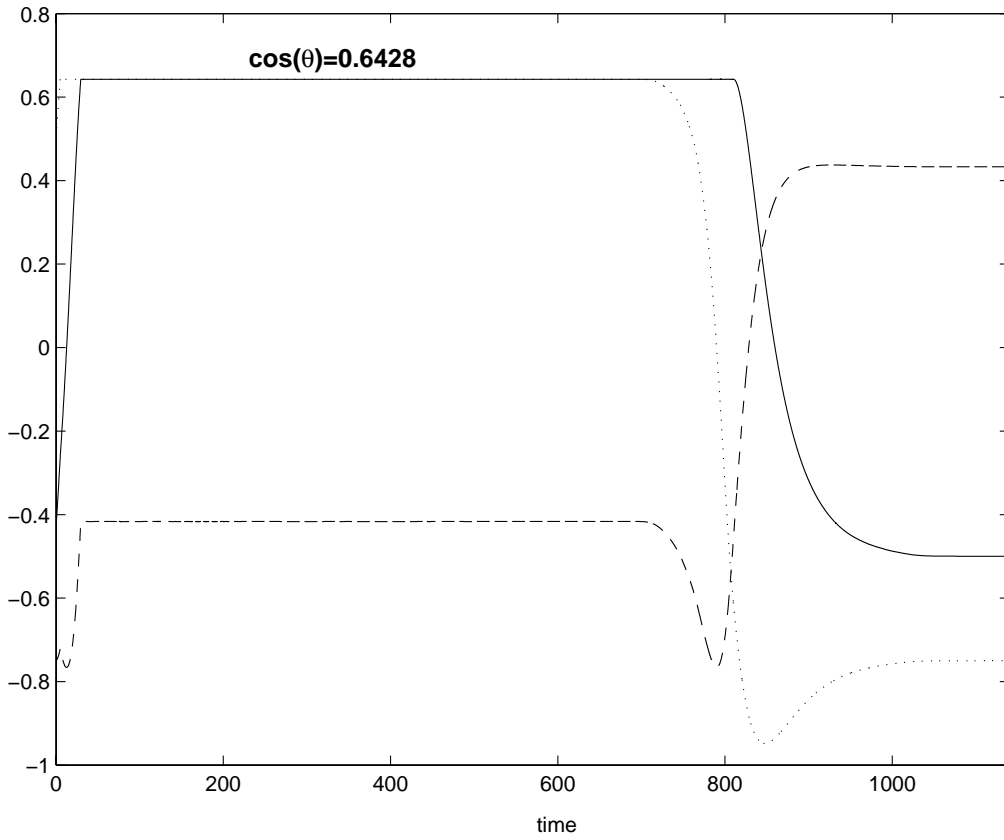


Figure 5: The inner products between inertially represented sensitive instrument vector $v(t)$ and thruster vectors $w_i(t)$ ($i = 1, 2, 3$): $v(t)^T w_1(t)$ (solid line), $v(t)^T w_2(t)$ (dotted line), and $v(t)^T w_3(t)$ (dashed line).

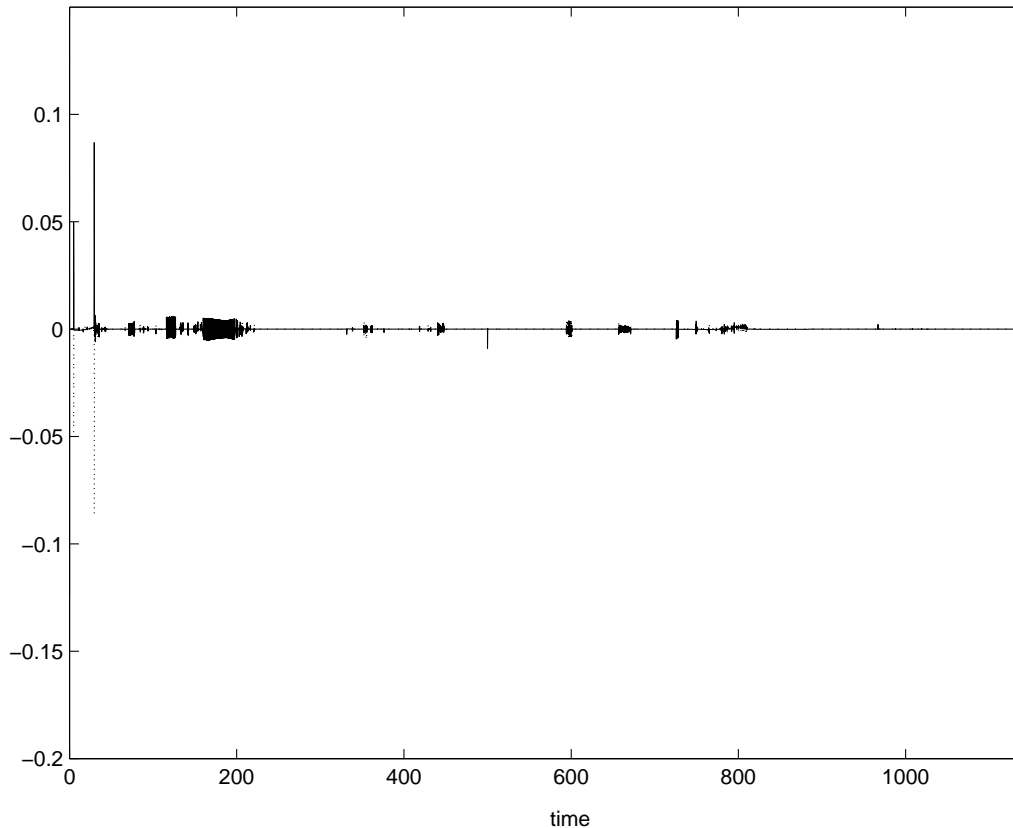


Figure 6: Control torques about the x -axis exerted on SC_1 (solid line) and SC_2 (dotted line).

and $v(t)^T w_1(t) \leq \cos \theta$ successively become active at 5.1 sec and 29.8 sec, and the corresponding values of $v(t)^T w_i(t)$ ($i = 2, 1$) stay constant at $\cos \theta = 0.6428$ until 699.3 sec and 810.8 sec, respectively. We note that the value of $v(t)^T w_3(t)$, where $t \in [29.8 \text{ sec}, 699.3 \text{ sec}]$, remains constant even when the corresponding constraint does not explicitly become active during the maneuver. Figure 6 depicts the control torques about the x -axis exerted on SC_1 (solid line) and SC_2 (dotted line).

Acknowledgments

The research of Y. Kim and M. Mesbahi was supported by NSF grant CMS-0093456 and by a grant from Jet Propulsion Laboratory, California Institute of Technology, under a contract with the

National Aeronautics and Space Administration. The research of G. Singh and F. Y. Hadaegh was carried out at the Jet Propulsion Laboratory, California Institute of Technology, under a contract with the National Aeronautics and Space Administration.

References

- ¹ Ahmed, A., Alexander, J., Boussalis, D., Breckenridge, W., Macala, G., Mesbahi, M., San Martin, M., Singh, G., and Wong, E., "Cassini Control Analysis Book," Jet Propulsion Laboratory, 1998.
- ² Collaudim, B., and Passvogel, Th., "The FIRST and Planck Carrier Missions: Description of Cryogenic Systems," Space Cryogenics Workshop, ESA Paper WPP-157, 1999, pp. 111–122.
- ³ Frakes, J. P., Henretty, D. A., Flatley, T. W., Markley, F. L., San, J. K., and Lightsey, E. G., "SAMPEX Science Pointing with Velocity Avoidance," *AAS/AIAA Spaceflight Mechanics Meeting*, AAS Paper 92-182, 1992, pp. 949-966.
- ⁴ Wen, J., and Kreutz-Delgado, K., "The Attitude Control Problem," *IEEE Transactions on Automatic Control*, Vol. 36, No. 10, 1991, pp. 1148–1161.
- ⁵ Kim, Y., and Mesbahi, M., "Quadratically Constrained Spacecraft Attitude Constrained Control Via Semidefinite Programming," *IEEE Transactions on Automatic Control*, Vol. 49, No. 5, 2004, pp. 731-735.
- ⁶ Hablani, H. B., "Attitude Commands Avoiding Bright Objects and Maintaining Communication with Ground Station," *Journal of Guidance, Control, and Dynamics*, Vol. 22, No. 6, 1999, pp. 759-767.
- ⁷ Spindler, K., "New Methods in On-board Attitude Control," *Advanced in the Astronautical Sciences*, Vol. 100, No. 2, 1998, pp. 111-124.
- ⁸ McInnes, C. R., "Large Angle Slew Maneuvers with Autonomous Sun Vector Avoidance," *Journal of Guidance, Control, and Dynamics*, Vol. 17, No. 4, 1994, pp. 875-877.
- ⁹ Wisniewski R., and Kulczycki, P., "Slew Maneuver Control for Spacecraft Equipped with Star Camera and Reaction Wheels," *Control Engineering Practice*, Vol. 13, No. 3, 2005, pp. 349-356.
- ¹⁰ Singh, G., Macala, G., Wong, E., and Rasmussen, R., "A Constraint Monitor Algorithm For the Cassini Spacecraft," *Proceedings of the AIAA Guidance, Navigation, and Control Conference*, AIAA, Reston, VA, 1997, pp. 272-282.
- ¹¹ Frazzoli, E., Dahleh, M. A., Feron, E., and Kornfeld, R., "A randomized attitude slew planning algorithm for autonomous spacecraft," *Proceedings of the AIAA Guidance, Navigation, and Control Conference*, AIAA, Montreal, Canada, 2001.
- ¹² Cheng, P., Frazzoli, E., and LaValle, S., "Improving the Performance of Sampling-Based Planners by Using a Symmetry-Exploiting Gap Reduction Algorithm," *Proceedings of the IEEE International Conference on Robotics and Automation*, New Orleans, CA, 2004, pp. 4362-4368.
- ¹³ Sorensen, A. M., "ISO Attitude Maneuver Strategies," *Proceedings of the American Astronautical Society*, AAS Paper 93-317, 1993, pp. 975-987.
- ¹⁴ Kim, Y., Mesbahi, M., and Hadaegh, F. Y., "Dual-spacecraft formation flying in deep space: optimal collision-free reconfigurations," *AIAA Journal of Guidance, Control, and Dynamics*, Vol. 25, No. 2, 2003, pp. 375-379.
- ¹⁵ Carrington, C., and Junkins, J., "Optimal nonlinear feedback control for spacecraft attitude maneuvers," *AIAA Journal of Guidance, Control, and Dynamics*, Vol. 9, No. 2, 1986, pp. 99–107.

- ¹⁶ Junkins, J., and Turner, J., “Optimal continuous torque attitude maneuvers,” *AIAA Journal of Guidance, Control, and Dynamics*, Vol. 3, No. 3, 1980, pp. 210–217.
- ¹⁷ Vadali, S., Kraige, L., and Junkins, J., “New results on the optimal spacecraft attitude maneuver problem,” *AIAA Journal of Guidance, Control, and Dynamics*, Vol.7, No. 3, 1984, pp. 378–380.
- ¹⁸ Gilbert, E., and Tan, K., “Linear systems with state and control constraints: the theory and application of maximal output admissible sets,” *Automatica*, Vol. 33, No. 12, 1997, 2103–2118.
- ¹⁹ Mayne, D., and Schroeder, W., “Robust time-optimal control of constrained linear systems,” *Automatica*, Vol. 33, No. 12, 1997, 2103–2118.
- ²⁰ Boyd, S. P., El Ghaoui, L., Feron, E., and Balakrishnan, V., *Linear Matrix Inequalities in System and Control Theory*, Society for Industrial and Applied Mathematics, Philadelphia, 1994.
- ²¹ Ben-Tal, A. and Teboulle, M., “Hidden convexity in some nonconvex quadratically constrained quadratic programming,” *Mathematical Programming*, Vol. 72, No. 1, 1996, 51–63.
- ²² Raymann, M. D., Varghese, P., Lehman, D. H., and Livesay, L. L., “Results From the Deep Space 1 Technology Validation Mission,” *Acta Astronautica*, Vol. 47, No. 1, 2000, pp. 475-487.
- ²³ SeDumi Website: <http://sedumi.mcmaster.ca/>
- ²⁴ Kuipers, J. B., *Quaternions and Rotation Sequences*, Princeton University Press, Princeton, New Jersey, 1999.